MINERALOGICAL MAGAZINE, SEPTEMBER 1982, VOL. 46, PP. 283-300

Ferromagnesian silicates in a differentiated alkaline complex: Kûngnât Fjeld, South Greenland

D. STEPHENSON

Institute of Geological Sciences, Murchison House, Edinburgh EH9 3LA

AND

B. G. J. UPTON

Grant Institute of Geology, University of Edinburgh, Edinburgh EH9 3JW

ABSTRACT. Kûngnât Fjeld is an intrusive complex resulting from three intrusive events involving trachyte, mafic trachyte and hawaiite magmas tapped successively from a single magmatic source. *In situ* differentiation produced gabbroic, syeno-gabbroic, syenitic, and quartz syenitic cumulates showing strong cryptic variation. Layered sequences of syenitic rocks total *c.* 3500 m. The compositional range is extended by late-stage minor intrusions of microsyenite and peralkaline granite. The principal cumulus minerals are feldspar ($Ab_{40}An_{60}$ to $Or_{45}Ab_{51}An_4$); olivine (Fo_{56} to Fo_1) and clinopyroxene ($Di_{70}Hd_{27}Ac_3$ to $Di_6Hd_{90}Ac_4$ followed by an abrupt change of trend towards $Di_3Hd_{78}Ac_{19}$ in the layered series and nearly pure aegirine in some peralkaline residues). Intercumulus phases are amphibole (hastingsite to ferro-edenite to ferro-actinolite in the layered series with riebeckite to arfvedsonite in some associated granites) and biotite ($annite_{31}$ to $annite_{98.5}$).

KÛNGNÂT FJELD, south Greenland, is a deeply dissected mountainous area composed of alkaline igneous rocks (Upton, 1960; Upton *et al.*, 1971). While dominantly syenitic, the alkaline complex exhibits an essentially continuous spectrum of rocks ranging from alkali olivine gabbro through ferrosyenogabbro, ferrosyenite, and quartz syenite to granitic residua, resulting from crystallization of magmas beneath a cover estimated at 4-5 km thickness. The complex is the westernmost known in the Gardar alkaline province (Emeleus and Upton, 1976) and was emplaced close to the southern edge of the Archaean craton at 1219 ± 16 Ma (Blaxland *et al.*, 1978).

Three principal intrusive events were involved in the emplacement of the complex (fig. 1): (i) an early western syenite stock intrusion was succeeded by (ii) an intersecting eastern stock. Both stocks had circular cross-sections with diameters of *c.* 3 km. They were followed by (iii) a gabbroic-syenogabbroic ring-dyke. The data supports a model involving three successive heaves of progressively higher temperature and less fractionated magma [(i) trachyte; (ii) mafic trachyte; and (iii) hawaiite] from a single underlying magmatic source. Each was emplaced in the upper crust by ring-faulting attendant on the subsidence of spalled sheets or large blocks of roofing rocks. The Kûngnât lithologies, extending from (just) nepheline-normative basic compositions to silica-oversaturated salic rocks, are held to represent a cogenetic series produced primarily by differentiation of an aluminous 'critically undersaturated' olivine basalt magma. Sr-isotopic studies (Blaxland, 1976) support the thesis that the three units were comagmatic. The initial $^{87}Sr/^{86}Sr$ ratio (0.7041 ± 0.0008) is, however, relatively high for a Gardar alkaline complex and Blaxland proposed the likelihood of some crustal contamination prior to differentiation.

Comparable emplacement of successively more primitive magmas during formation of a Gardar alkaline complex has been noted at South Qôroq (Stephenson, 1972). Such a sequence can be explained in terms of magma batches which had successively higher ascent rates through the lithosphere and which consequently show less fractionated characteristics with increasing youth. Alternatively, the magma batches could have arisen from the tapping of a compositionally stratified magma body, with fractions derived from progressively deeper levels. Because of independent evidence for the existence of such compositionally stratified magma bodies in Gardar times (Bridgwater and Harry, 1968), there is some reason to favour this second hypothesis. The development of such a magma body, through crystal fractionation processes, has been outlined by Cox *et al.* (1979) for the Aden volcano.

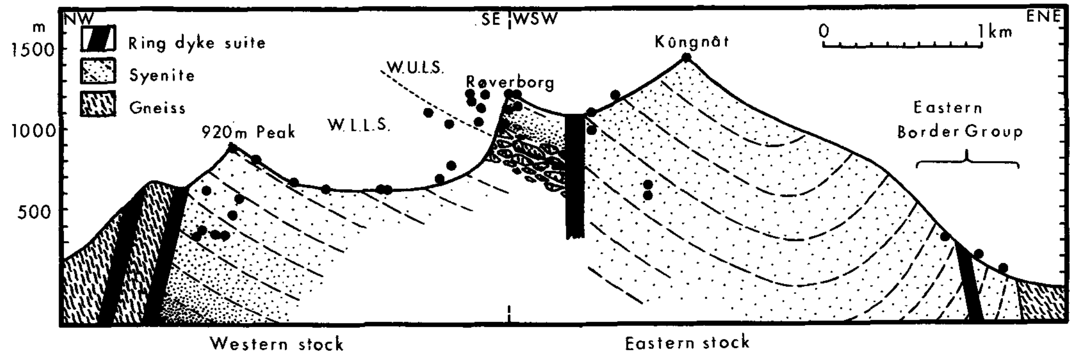

FIG. 1. Generalized cross-section in an approximate west-east direction across the Kûngnât Fjeld Complex. The raft of xenoliths beneath Røverborg is indicated diagrammatically. Samples used for mineral analyses are shown projected on to the section in equivalent positions relative to the igneous layering structures, in the manner described in the text. (WLLS and WULS; Western Lower and Upper Layered Series)

The time intervals separating the three intrusions are believed to have been brief so that the second and third intrusions were emplaced in rocks that were still at relatively high temperatures. Each intrusion underwent *in situ* fractionation producing cumulitic suites, and basinal disposition of mafic stratification is shown by both syenitic stocks. Exposures in the earlier (western) stock reveal some 1800 m of layered syenites divided by a sub-horizontal raft of gneiss and metavolcanic xenoliths (believed to be detached from the magma chamber roof) into an upper layered series (*c.* 400 m) and a lower layered series (*c.* 1400 m). Both series show a generalized upward sequence involving decrease in Fe, Mg, Ca, Ti, and P and concomitant increase in Si, Al, Na, and K (Upton, 1960). The lower layered series grades up from mafic ferrosyenites to leucocratic quartz syenites. Cross-cutting sheets of peralkaline granites are regarded as filter-pressed residua which continued to be expelled until after the emplacement of all of the major units. The upper layered series shows gradation from syenites to extremely leucocratic (perthositic) quartz syenites.

The eastern stock is principally composed of mesocratic syenites; while generally more homogeneous and less differentiated than the western stock it does show some variation to quartz syenite derivatives. Upton (1960) divided the intrusion into an eastern marginal border group (with steep, sub-vertical layering) partly enclosing an inner layered series with shallower dips. No simple relationship between bulk composition and height in the inner layered series (or distance from the margin in the border group) was recognized.

The ring-dyke, rarely over 100 m broad and virtually complete through 360°, is mostly free from layering but does occasionally show cumulate textures. Variation along strike from olivine gabbro to ferrosyenogabbro was ascribed by Upton to filter-pressing effects attendant on the eccentric collapse of the rocks enclosed by the ring-dyke.

Within the Gardar province, the alkaline rock series seen at Kûngnât Fjeld is closely similar to those seen in the rather younger Klokken (Parsons, 1979) and Tugtutôq Younger Giant Dyke (Upton and Thomas, 1980) complexes.

Petrography

The gabbros and syenogabbros are composed of feldspars, olivines, clinopyroxenes, Fe-Ti oxides, apatites, and biotites. The feldspars are strongly zoned and show plagioclase core compositions from An_{60} to about An_{20}, while the modal amount of outer-zone cryptoperthites increases with differentiation. Clinopyroxenes, interstitial in the more primitive gabbros, become idiomorphic and acquire cumulus status in the ferrosyenogabbros. The modal amounts of biotite, Fe-Ti oxide (variably exsolved and oxidized titaniferous magnetites) and apatite increase to a maximum in the ferrosyenogabbros.

In the syenite stocks primary plagioclase cores are absent in the feldspars; these show unmixed textures varying from cryptoperthite to antiperthite and perthite. The bulk compositions correspond to anorthoclases and sanidines, the K/Ca ratios increasing with fractionation. All the rocks of the complex, with the exception of some late peralkaline transgressive microgranites, appear to have formed under hypersolvus conditions. Bulk analysis of the feldspars (and Fe-Ti oxides) by microprobe is made difficult by the exsolution textures commonly exhibited and a thorough revised study remains desirable. However, a general survey of bulk feldspar compositions in the Kûngnât complex, using partial analyses (flame-photometric for Na and K; optical-emission spectroscopy for Ca, Sr, Ba, Rb, and Li) on separated feldspar fractions (Upton, 1960) showed the feldspars in the syenites to range from $Or_{29}Ab_{58}An_{10.5}Cn_{1.5}$ to $Or_{45}Ab_{51}An_4$. Sr enrichment is at a maximum in the sodic plagioclase of the ring-dyke while maximum Ba levels were attained in the antiperthites (presumed originally anorthoclase) of the eastern syenites.

Cumulus olivine, clinopyroxene, Ti-magnetite, and apatite are also present in the layered syenites, and are concentrated in the mafic layers and schlieren. The modal abundance of these minerals shows a generalized upward decline through the western layered syenites culminating in the leucocratic perthosites at the highest preserved levels in the western upper layered series.

Amphiboles, much of the mica (biotite), and quartz are confined to interstitial (intercumulus) rôles in the syenites. Some of the biotite, however, may have been produced by sobsolidus growth around Ti-magnetite crystals. In the upper parts of the western layered series amphibole and biotite become the principal ferromagnesian minerals as the modal amount of cumulus mafic minerals diminishes.

The apatites of the complex show significant compositional change with increasing differentiation: Ca, P, Sr, and Cl decrease while Si, Fe, Na, Y, *REE*, and F rise (Hill and Upton, in prep.).

Zircon, calcite, siderite, and fluorite occur as accessory minerals in some of the more highly fractionated syenites. Small quantities of pyrrhotine, chalcopyrite, and pentlandite occur in the ring-dyke suite and in the less fractionated syenites.

Astrophyllite (Macdonald and Saunders, 1973) and thorite appear to be confined to late peralkaline acid sheets associated with the western lower layered syenites. Ilmenite (moderately manganiferous with up to 5% MnO) appears as the sole Fe-Ti oxide mineral in the late peralkaline sheets. Radiating sprays of aegirine and, or, astrophyllite surrounding anhedral relict ilmenite crystals suggest the likelihood of a low-temperature reaction relationship involving this mineral and alkali-rich residual fluid.

Aenigmatite, present in some Gardar Si-oversaturated complexes, has not been found in the Kûngnât rock suite.

The change from mildly silica-undersaturated parental magmas to silica-oversaturated magmas is believed to be related to strong iron enrichment in the middle stages of differentiation, followed by precipitation of silica-free minerals, in particular titaniferous magnetite. The transition from peraluminous condition to peralkaline condition is attributed to separation of Ca-bearing feldspars (Upton *et al.*, 1971), and is only apparent in the final residues yielded by the western lower layered series.

Analytical techniques

All analyses were made on electron probe microanalysers manufactured by 'Cambridge Scientific Instruments'. Early analyses were made on the Geoscan 2 of Durham University but the majority were made on the Microscan 5 of Edinburgh University using crystal spectrometry. Later analyses, mostly of the late differentiates, were made using energy dispersive spectrometry on the Microscan 5. In all cases the standards used were of pure elements, oxides or simple silicate compositions. Corrections were made for dead time, atomic number, absorption, and fluorescence, using computer programs based upon the methods of Sweatman and Long (1969). Representative analyses are shown in Tables I and II.

Mineralogy

Olivines. Olivine remained in equilibrium with all but the most highly differentiated magmas. It is abundant in the ring-dyke suite and in the lowest levels of the western lower layered series but olivine has a more sporadic distribution in higher levels of the western centre and in the eastern centre, where its occurrence is often restricted to mafic layers. In the more highly fractionated quartz syenites of the western upper layered series olivine shows signs of instability and oxidation and none is seen in the granitic residua.

The total variation in olivine compositions (Fo_{56} to Fo_1) is illustrated in fig. 2. Although Fo_{56} is the most magnesian olivine yet recorded in any of the Gardar central complexes, a range of Fo_{65} to Fo_4 has been noted for the somewhat similar rock suite composing the Tugtutôq Younger Giant Dyke Complex (Upton and Thomas, 1980). The olivines of the Kûngnât ring-dyke suite range from Fo_{56} to Fo_{21}. While in the context of the Gardar alkaline complexes they are relatively magnesian, their Fe-rich nature suggests that the ring-dyke magmas are themselves products of strong fractionation. Eastern border group and eastern layered series compositions fall within the same range of Fo_{18} to Fo_6 supporting the conclusion of Upton (1960) that the two are contemporaneously evolved from a single batch of magma. Western lower layered series compositions range from Fo_6 to Fo_1. Analyses are not available from the western upper layered series where compositions would be expected to be close to those at the top of the western layered series. Zoning in individual crystals is usually slight (<1 % Fo) and individual samples rarely exhibit a total variation of more than 3 % Fo.

Overall, the analyses form a smooth, continuous trend of Fe enrichment with a gradual, though slight, Mn enrichment. The trend is colinear with trends from most other Gardar suites such as Ilímaussaq (Larsen, 1976), Klokken (Parsons, 1979), Tugtutôq Younger Giant Dyke (Upton and Thomas, 1980), Hviddal and Central Tugtutôq (Stephenson and Upton, unpubl.). Mn is high compared with olivines from most igneous suites elsewhere in the world but the extreme Mn enrichment of the various Igaliko centres of the Gardar province (Stephenson, 1974; Chambers, 1976; Powell, 1978; and Jones, 1980) and the Oslo region (Neumann, 1976) is lacking. Excluding the Igaliko centres, no significant differences are observed between olivine trends from silica-oversaturated and silica-undersaturated Gardar suites such as are observed in trends of several other mineral phases. This is probably due to the fact that olivine is an early-crystallizing phase in both types of suite whose crystallization is largely complete before other chemical and mineralogical parameters become divergent. Such divergence is associated with a variation in the onset of Na enrichment in coexisting pyroxenes which in all the Gardar suites is intimately associated with instability, oxidation, and eventual disappearance of fayalite. The long stability range of olivine in the Kûngnât Complex (as in most other Gardar silica-oversaturated suites) is thus associated with the relatively Na-poor pyroxene trend which starts to show Na enrichment only in the western upper layered series syenites.

Of the minor elements, only Ca occurs in significant proportions, ranging from 0.07 to 0.38 % CaO (<0.2 wt. % Ca) with no systematic variation through the series. Such values are close to the 'normal' limit for plutonic olivines of 0.1 wt. % Ca proposed by Simkin and Smith (1970) and similar values are found in olivines from other Gardar silica-oversaturated suites (e.g. Upton and Thomas, 1980). This contrasts with the abnormally high

TABLE I. *Representative analyses of mafic silicates from ring-dyke and layered series*

	1	2	3	4	5	6	7	8	9	10
SiO_2	35.53	30.06	51.22	49.32	48.82	44.41	38.95	49.89	36.88	34.86
TiO_2	0.04	—	1.33	0.21	0.28	0.24	1.47	0.13	4.56	2.48
Al_2O_3	0.07	0.06	2.67	0.51	0.26	6.43	9.60	0.71	14.54	10.68
Fe_2O_3*	—	—	1.60	1.60	6.26	—	—	—	—	—
FeO	39.36	67.22	8.12	26.56	23.66	24.81	29.32	36.68	12.41	36.52
MnO	0.68	2.60	0.19	1.04	0.65	0.39	0.67	1.27	—	0.14
MgO	24.27	0.44	12.82	1.05	0.44	7.54	2.05	0.26	14.91	1.49
CaO	0.16	0.11	21.51	19.91	17.21	10.01	10.40	8.74	—	—
NaO	—	—	0.62	0.62	2.43	2.35	2.69	1.27	0.30	0.06
K_2O	—	—	—	—	—	1.24	1.49	0.30	9.34	8.46
Total	100.11	100.49	100.08	100.82	100.01	97.42	96.64	99.25	92.94	94.69
Atomic proportions										
Si	1.007	1.007	1.912	1.995	1.987	6.963	6.401	7.958	5.588	5.868
Ti	0.001	—	0.037	0.006	0.009	0.028	0.182	0.016	0.520	0.314
Al	0.002	0.002	0.118	0.024	0.012	1.189	1.860	0.134	2.597	2.120
Fe^{3+}	—	—	0.045	0.049	0.192	—	—	—	—	—
Fe^{2+}	0.933	1.883	0.254	0.899	0.805	3.254	4.030	4.894	1.573	5.142
Mn	0.016	0.074	0.006	0.036	0.022	0.052	0.093	0.172	—	0.020
Mg	1.025	0.022	0.713	0.063	0.027	1.762	0.502	0.062	3.367	0.374
Ca	0.005	0.004	0.861	0.863	0.751	1.682	1.832	1.494	—	—
Na	—	—	0.045	0.049	0.192	0.715	0.858	0.393	0.088	0.020
K	—	—	—	—	—	0.248	0.312	0.061	1.806	1.817
O	4.000	4.000	6.000	6.000	6.000	23.000	23.000	23.000	22.000	22.000

1 olivine (86186) Ring-dyke
2 olivine (81108) WLLS
3 pyroxene (86186) Ring-dyke
4 pyroxene (81108) WLLS
5 pyroxene (126877) WLLS/WULS
6 amphibole (126850) EBG
7 amphibole (126868) WLLS
8 amphibole (126873) WULS
9 biotite (58301) Ring-dyke
10 biotite (81103) WULS

* Fe_2O_3 in pyroxenes calculated from Fe^{3+} = Na, FeO by difference. FeO in other phases = total Fe.

Sample numbers refer to the Geological Survey of Greenland collection.

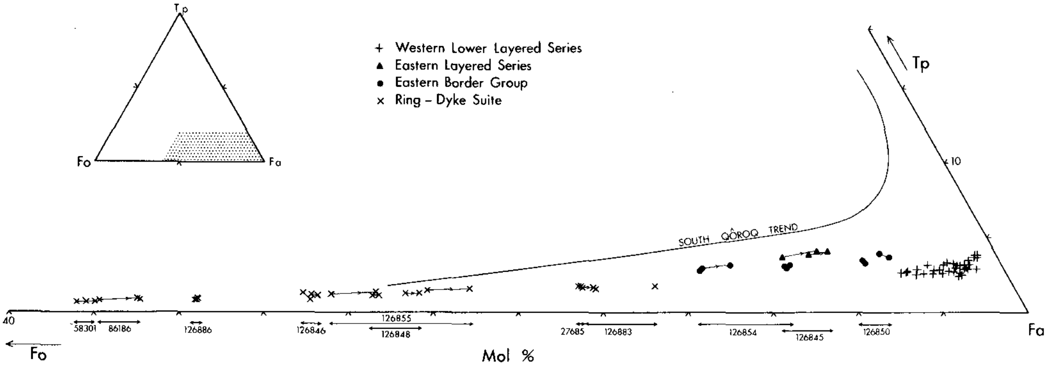

FIG. 2. Olivine analyses from the Kûngnât Complex. Ranges of individual rocks are shown for the ring-dyke suite and Eastern Centre. The Mn-rich trend from the South Qôroq Centre of the Gardar Province (Stephenson, 1974) is shown for comparison.

TABLE II. *Representative analyses of mafic silicates from late stage granitic sheets*

	1	2	3	4	5	6	7	8	9	10
SiO_2	52.76	52.84	47.02	49.88	51.47	50.35	38.99	37.37	35.90	36.36
TiO_2	0.58	1.38	1.27	0.81	1.40	0.62	2.82	3.10	10.50	8.71
ZrO_2	—	—	—	—	—	—	—	—	1.02	1.14
Al_2O_3	0.24	0.37	2.51	1.61	0.34	0.60	7.46	7.61	0.82	0.76
Nb_2O_3	—	—	—	—	—	—	—	—	0.81	3.40
Fe_2O_3*	33.11	31.46	—	—	—	—	—	—	—	—
FeO	—	—	35.47	35.15	31.26	33.93	34.46	38.52	35.84	35.34
MnO	—	0.10	1.00	0.62	3.00	0.82	0.76	—	1.23	2.10
MgO	—	0.02	—	0.17	0.77	—	1.96	0.31	—	—
CaO	1.37	0.12	5.37	0.18	0.26	0.42	—	—	0.34	0.68
ZnO	—	—	—	—	—	—	—	—	0.67	0.23
Na_2O	13.33	13.84	4.64	8.89	8.00	8.98	0.85	0.60	3.08	2.48
K_2O	—	—	0.95	1.31	1.46	1.69	9.05	8.48	5.67	5.52
Total	101.39	100.13	98.21	98.63	97.95	97.41	96.34	96.00	95.88	96.71
Atomic proportions										
Si	2.163	2.012	7.630	7.987	8.197	8.157	6.383	6.251	7.211	7.257
Ti	0.018	0.040	0.155	0.098	0.168	0.075	0.348	0.390	1.586	1.307
Zr	—	—	—	—	—	—	—	—	0.100	0.111
Al	0.012	0.017	0.479	0.304	0.064	0.114	1.440	1.501	0.195	0.180
Nb	—	—	—	—	—	—	—	—	0.074	0.307
Fe^{3+}	1.032	0.901	—	—	—	—	—	—	—	—
Fe^{2+}	—	—	4.815	4.707	4.163	4.597	4.575	5.388	6.023	5.898
Mn	—	0.003	0.139	0.085	0.406	0.113	0.105	—	0.209	0.356
Mg	—	0.001	—	0.041	0.183	—	0.609	0.078	—	—
Ca	0.061	0.005	0.934	0.031	0.045	0.073	—	—	0.073	0.146
Zn	—	—	—	—	—	—	—	—	0.100	0.034
Na	1.068	1.002	1.459	2.760	2.469	2.820	0.272	0.196	1.198	0.961
K	—	—	0.197	0.267	0.298	0.349	1.890	1.811	1.455	1.405
O	6.000	6.000	23.000	23.000	23.000	23.000	22.000	22.000	26.000	26.000

1	pyroxene (86197B)	5	amphibole (86191B)	8	biotite (86159)
2	pyroxene (86157)	6	amphibole (86197B)	9	astrophyllite (86184)
3	amphibole (86176)	7	biotite (86154)	10	astrophyllite (86191B)
4	amphibole (86184)				

* Fe_2O_3 in pyroxenes calculated from Fe^{3+} = Na or total Fe, whichever lowest. FeO in other phases = total Fe.

Sample numbers refer to the Geological Survey of Greenland collection.

values (up to 1% CaO) reported from Gardar silica-undersaturated suites (Stephenson, 1974; Chambers, 1976; Larsen, 1976). The contrast supports the view that Ca is incorporated into the olivine lattice at a late stage, i.e. after the silica-oversaturated and silica-undersaturated suites have started to evolve along different mineralogical and chemical paths.

Al is present in very small amounts (0.01 to 0.14% Al_2O_3) throughout the suite and Ti (up to 0.17% TiO_2) is detected in a few samples.

Clinopyroxenes. In the most primitive gabbros the pale pinkish augite has a sub-ophitic relationship to the plagioclase and olivine. In the more differentiated (syeno-gabbroic) parts of the ring-dyke, pyroxene increases in modal abundance, assumes a more idiomorphic habit and joins olivine and plagioclase as a cumulus mineral.

In the lowest exposed levels of the western lower layered series the pyroxenes are idiomorphic (cumulus) crystals showing colour zonation from pink-grey cores to pale green margins. The zoning is frequently patchy suggesting some irregular late-stage replacement. With increasing stratigraphical height the pink-grey cores are lost and the pyroxenes become green throughout; colour intensity (and pleochroism) increases towards the margins as Fe enrichment increases. Such green and pleochroic pyroxenes characterize the highest quartz syenites accessible beneath the xenolithic raft. They are of hedenbergitic composition becoming slightly sodic only in extreme examples comparable to similar green hedenbergites from Klokken (Parsons, 1979) and Coldwell, Ontario (Mitchell and Platt, 1978).

Pyroxenes of the western upper layered series are pale green, slightly pleochroic idiomorphic prisms, up to 3 mm long. In the eastern centre pyroxenes range from pinkish augite to green non-pleochroic hedenbergite but do not show a systematic compositional progression.

A decrease in the modal olivine/pyroxene ratio throughout the whole rock suite (olivine gabbro to quartz syenite) accompanies the overall decrease in ferromagnesian mineral content. However, pyroxene shows less tendency than olivine to concentrate exclusively in mafic layers and hence is present in all rocks selected for analysis.

Major element variation is shown in fig. 3*a* where a smooth, continuous trend is observed from $Di_{70}Hd_{27}Ac_3$ to $Di_3Hd_{78}Ac_{19}$ with an abrupt turn at $Di_6Hd_{90}Ac_4$ towards Na enrichment. Compositions more sodic than Ac_{19} do not occur in the layered series, giving rise to a marked compositional break between pyroxenes of the quartz syenites and those of the late granitic sheets, which are almost pure aegirine. In the system wollastonite–enstatite–ferrosilite (not shown) the trend is from $Wo_{45}En_{40}Fs_{15}$ to $Wo_{45}En_2Fs_{53}$.

As with the olivines, the pyroxenes show variation both within and between the various units although, unlike the olivines, there is a slight overlap of compositions between the units. This may simply reflect a greater degree of intercumulus growth in the pyroxenes, extending the ranges towards slightly more fractionated compositions. The eastern border group and eastern layered series correspond exactly in compositional range. The upper parts of the western lower layered series (laminated and unlaminated groups) do have a significant overlap but show a general upward trend towards increasing Hd. The abrupt onset of Na enrichment at Hd_{90} corresponds exactly with a sharp junction (with no overlap) between compositions of the western lower layered series and western upper layered series. This emphasizes the division into two separately evolving masses of magma in the western centre brought about by a sinking and fragmenting raft of roofing materials (Upton, 1960). The only significant departure from this scheme occurs in sample no. 126880 which is a pegmatitic facies within the western upper layered series. Pyroxenes from this rock exhibit a much wider range than is usual, covering the whole range observed in the western lower layered series but with a slightly increased Na content.

Pyroxene zoning as a result of intercumulus growth is common in the syenite cumulates. Individual crystals can exhibit the total range seen in a particular sample with zonal variations of up to 15% Hd in the eastern syenites and 5% Hd or Ac in the western centre.

The overall trend (augite → hedenbergite → sodic hedenbergite) (fig. 3*a*) is typical of other silica-oversaturated suites from the Gardar Province and is in marked contrast to pyroxene trends from Gardar silica-undersaturated suites (augite → aegirine-augite → aegirine). Comparative, generalized trends from the Gardar Province are shown in fig. 3*b* and Stephenson (1972) and Larsen (1976) have published diagrams showing a similar effect in suites from elsewhere. The exception to this pattern occurs in the agpaiitic, undersaturated parts of the Ilímaussaq Complex where the pyroxene trend passes through hedenbergite before developing a full series of exceptionally Mg-poor aegirine-augites and aegirines. This anomaly has been explained by Larsen (1976) in terms of the low MgO content and low oxygen fugacity of the Ilímaussaq magma.

Mitchell and Platt (1978) suggest that Na enrichment of pyroxene is a function of peralkalinity and is independent of silica saturation of the liquid. Support for this may be found in the Oslo Province

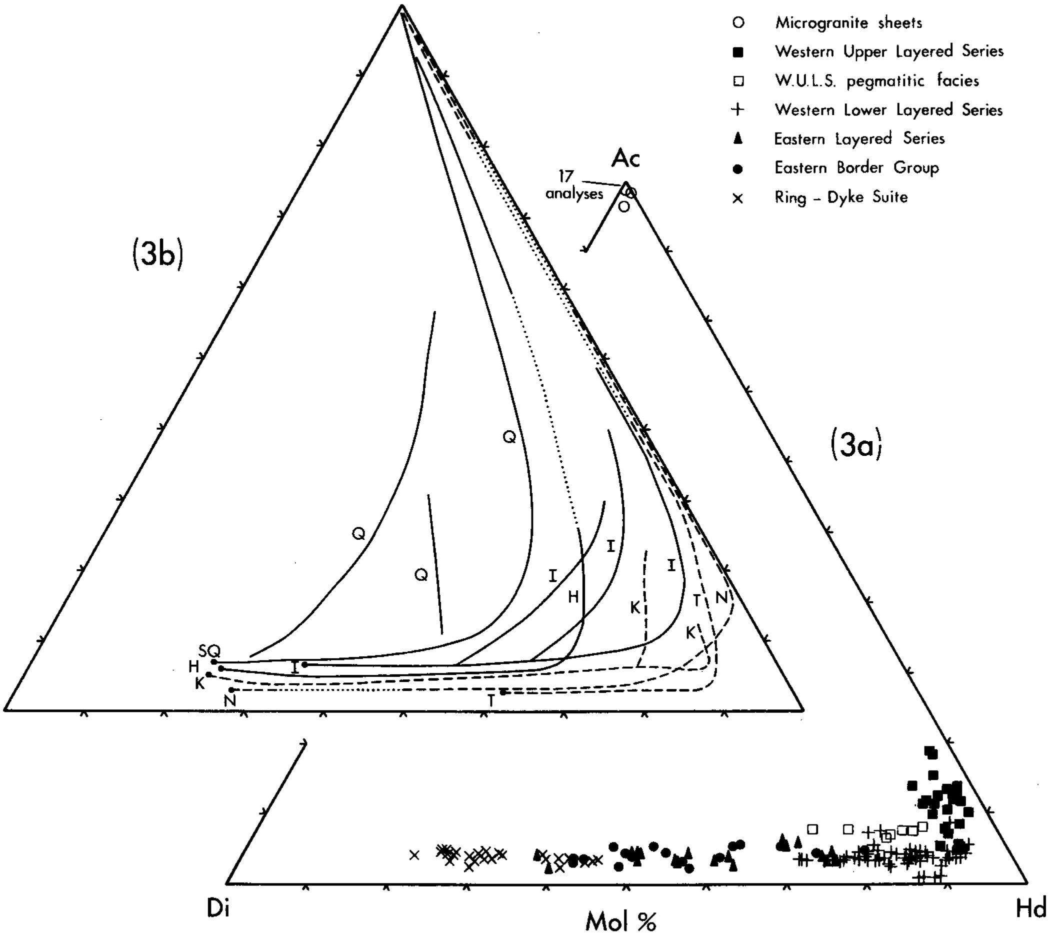

FIG. 3. (*a*) Pyroxene analyses from the Kûngnât Complex. (*b*) Generalized pyroxene trends from other Gardar complexes. Solid lines are from silica-undersaturated suites and dashed lines from silica-oversaturated suites. Dotted lines indicate breaks in the sequences. Q = South Qôroq Centre (Stephenson, 1972); I = Igdlerfigssalik Centre (Powell, 1978); H = Hviddal Dyke (Stephenson and Upton, unpubl.; K = Klokken Complex (Parsons, 1979); N = Nunarssuit-Alangorssuaq (Anderson, 1974); T = Tugtutôq Central Complex (Stephenson and Upton, unpubl.). The Ilímaussaq trend (Larsen, 1976) is omitted for clarity. This trend shows a gap; the trend from the less-differentiated rocks runs parallel to the Di-Hd join and is coincident in part with that of the Kûngnât syenites. The trend for the more differentiated Ilímaussaq rocks lies very close to the Hd-Ac join. The inflexion in the Ilímaussaq trend is almost coincident with that of the Kûngnât trend.

(Neumann, 1976) where alkali pyroxenes from both over- and under-saturated plutonic suites fall on a single Fe^{2+}-poor trend. Neumann points out that 'in the Oslo region, sodic pyroxenes are only found in rocks with agpaitic indexes (Na + K/Al) greater than 1.0'. She also describes reasonable correlation between Na content of pyroxenes and Na/(Na + Ca) in the bulk rock.

Quantitative attempts to relate the type of pyroxene trend to bulk rock peralkalinity (or to any other bulk-chemical parameter) in the Gardar suites have been unsuccessful. However, it is appropriate to consider the peralkalinity of the intercumulus liquid, which is more likely to influence the later stages of pyroxene crystallization than is bulk-rock composition. The intercumulus liquid may become peralkaline at an earlier stage of crystallization in the undersaturated suites than in the oversaturated, irrespective of whether or not the rocks are peralkaline in bulk terms (the majority of Gardar suites are not appreciably peralkaline). We concur with Mitchell and Platt in suggesting that silica saturation does not necessarily have a direct influence on Na enrichment in pyroxenes and that the chemical parameters, in particular peralkalinity, provide a more likely control. Thus, the contrasting trends observed in the Gardar suites probably reflect a secondary correlation due to an interdependence between silica saturation and other chemical and mineralogical factors.

The close correlation in Kûngnât rocks between the onset of Na enrichment in pyroxenes and fayalite instability is also apparent in most other Gardar suites. Fayalite thus remains stable throughout a longer crystallization interval in Si-oversaturated suites (and in Ilímaussaq) than in Si-undersaturated suites. The implication of this observation is that when Na enrichment of pyroxene commences, fO_2 [which has hitherto been falling steadily with decreasing temperature along a curve close to the fayalite-magnetite-quartz buffer (FMQ)] is lifted above the buffer curve and out of the fayalite-stability field. Such an observation was also made by Nash and Wilkinson (1970) and Larsen (1976). It is not certain whether this slight decrease in slope of the oxygen buffer curve is a cause or an effect of Na enrichment in pyroxenes. Accounts relating temperature, oxygen fugacity, silica activity, and appropriate mineral stability fields in similar rocks may be found in Nash and Wilkinson (1970), Neumann (1976), and Mitchell and Platt (1978).

In the more highly fractionated Kûngnât rocks, pyroxene crystallization was generally terminated by a reaction relationship in which an alkali amphibole became the stable phase (see next section). Amphibole then remained stable until the very late stages of crystallization when pyroxene crystallization recommenced as nearly pure aegirine, often as the only mafic phase, but also often accompanied by, or enclosing, riebeckitic amphibole. Ernst (1962) and Bailey (1969) have shown that acmite can become stable in place of alkali amphibole at low temperatures even in the presence of excess water provided that there is excess Na-silicate in the liquid and that the oxygen fugacity lies above the fayalite-magnetite-quartz buffer. Such conditions are thus inferred for the residual fluids expelled in the final stages of consolidation of the western lower layered series magmas. It may be significant that only the latest (lowest temperature) microgranites contain aegirine, whereas slightly earlier (presumed higher temperature) granites do not.

Significant minor elements in the pyroxenes are Mn, Al, and Ti. Mn behaves similarly to Fe^{2+}, ranging from 0.17% MnO in the gabbros to a maximum of 1.11% MnO at the top of the western lower layered series and decreasing slightly with Na-enrichment in the western upper layered series. Both Al and Ti fall continuously (fig. 4) from high values in the more magnesian pyroxenes of the gabbros to almost zero in the most fractionated pyroxenes of the western upper layered series quartz syenites (Al_2O_3, 3.25 to 0.07%; TiO_2, 1.78 to 0.07%). Individual crystals from the ring-dyke suite and eastern centre commonly show an increase in Al and Ti from core to rim contrary to the overall decreasing trend. Such anomalies are not observed in the western centre (fig. 4).

In the less-differentiated rocks (ring-dyke suite and eastern centre) the behaviour of Al and Ti is almost identical to that found in other Gardar Complexes. However, the continuing decline in concentration towards zero, which is observed in the Kûngnât western centre, Klokken (Parsons, 1979) and Central Tugtutôq (Stephenson and Upton, unpubl.) does not occur in the pyroxenes from the silica-undersaturated complexes of Igaliko (Stephenson, 1972), Ilímaussaq (Larsen, 1976), and Hviddal (Stephenson and Upton, unpubl.). In these latter, the values level off and even increase slightly in the more fractionated pyroxene compositions. It would seem that in the less-differentiated Kûngnât rocks, most of the pyroxene Al is in tetrahedral sites but that Si gradually increases, excluding Al which eventually falls to zero in the more fractionated pyroxenes. However, in the silica-undersaturated suites the presence of excess Na, relative to iron, in the pyroxenes permits formation of the jadeite molecule ($NaAlSi_2O_6$), with Al entering the octahedral Y-sites, possibly accompanied by Ti, to form complex Na-Ti end-members (Larsen 1976, Table IV).

*Amphiboles.** Primary amphibole is absent from the ring-dyke suite but is prominent as an intercumulus mineral in syenites of the eastern and western centres, occurring interstitially or as a reaction rim around pyroxene. The amphiboles range from browns and brownish-greens in the ferrosyenites to bluish-greens in the syenites and quartz syenites. Analyses show them to be calcic amphiboles mostly falling within the range hastingsite ($NaCa_2Fe_4^{2+}Fe^{3+}Si_6Al_2O_{22}(OH)_2$), ferro-edenite ($NaCa_2Fe_5^{2+}Si_7AlO_{22}(OH)_2$) to slightly alkaline ferro-actinolite ($Ca_2Fe_5^{2+}Si_8O_{22}(OH)_2$). Amphiboles from some of the more highly fractionated quartz syenites of western Kûngnât (containing slightly sodic pyroxenes) are more alkaline with

---

* Since the preparation of this manuscript, Giret *et al.* (1980. *Can. Mineral.* **18**, 481–95) have documented contrasting amphibole trends and coupled ionic substitutions almost identical to those of the Gardar Province, from a range of silica-oversaturated and silica-undersaturated, oceanic and continental alkaline rock suites.

compositions falling between ferro-actinolite and ferro-richterite $(NaCaNaFe_5^{2+}Si_8O_{22}(OH)_2)$. Upton (1960) noted optical evidence that the outer zones of such amphiboles were riebeckite but this lacked analytical confirmation. In fact, the amphiboles of granitic sheets associated with the western lower layered series, which appear riebeckitic on optical evidence, yield analyses close to pure arfvedsonite $(NaNa_2Fe_4^{2+}Fe^{3+}Si_8O_{22}(OH,F)_2)$. Rowbotham (1973) termed them 'riebeckite-arfvedsonite'.

The amphibole analyses are plotted in the system (Na + K)-Mg-Fe (fig. 5). This diagram permits some comparison with the pyroxene trends (fig. 3*a*) though it should be noted that, owing to the difficulty in allocating Fe^{3+}/Fe^{2+} stoichiometrically from probe analyses, total Fe must be used in the plot. (In the case of the Kûngnât analyses this problem is not serious since Fe^{2+} is very close to total Fe in the pyroxenes and probably in most amphiboles.) Most of the analyses lie on a trend which is initially comparable to that of the corresponding pyroxenes in terms of Fe/Mg but with a much higher content of total alkalis. This relationship holds for the less-fractionated compositions found in the eastern centre. However, amphiboles from the western centre show a marked contrast in trend from that of their corresponding pyroxenes; whereas the latter rises towards alkali enrichment and iron depletion (fig. 3*a*), the amphiboles show a downward trend towards Fe^{2+} enrichment and alkali depletion (fig. 5). This part of the trend cannot be represented by a single line common to all of the analysed rocks. Each individual rock forms a separate trend towards Fe enrichment, the starting point of which depends upon the composition of the pyroxene immediately preceding amphibole crystallization. This is particularly well seen in sample 126877 in which the pyroxene compositions exhibit alkali enrichment, but in which the amphiboles start relatively alkali rich with compositions close to ferro-richterite (alkalis inherited in part from the pyroxene) and then trend towards ferro-actinolite with alkali depletion and iron enrichment.

Most Gardar suites show a reaction relationship between pyroxene and alkali amphibole (Stephenson, 1972; Larsen, 1976) which occurs in response to falling temperature and f_{O_2} (close to FMQ) and rising P_{H_2O} in the liquid due to the prolonged history of crystallization of anhydrous phases (Ernst, 1962, 1966; Charles, 1975). The stage at

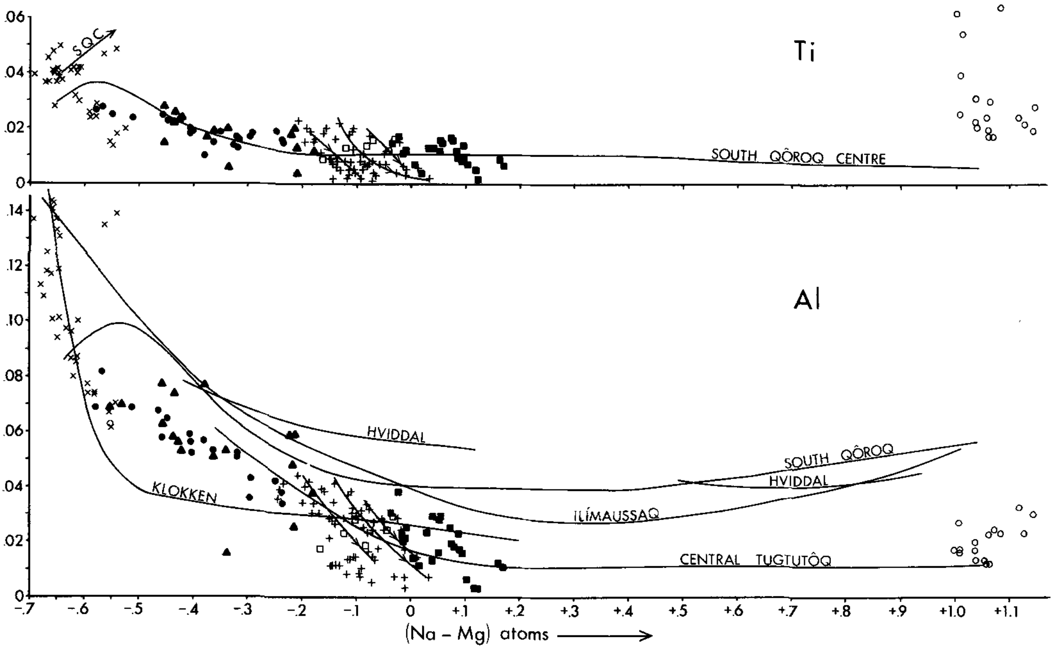

FIG. 4. Al and Ti in Kûngnât pyroxenes relative to the alkali pyroxene fractionation index (Na–Mg atoms). Symbols as for fig. 3*a*. Arrows indicate generalized trends from individual rocks. Overall Al trends are shown from the silica-undersaturated suites of South Qôroq (Stephenson, 1972), Ilímaussaq (Larsen, 1976), and Hviddal (Stephenson and Upton, unpubl.); and the silica-oversaturated suites of Klokken (Parsons, 1979) and Tugtutôq Central Complex (Stephenson and Upton, unpubl.).

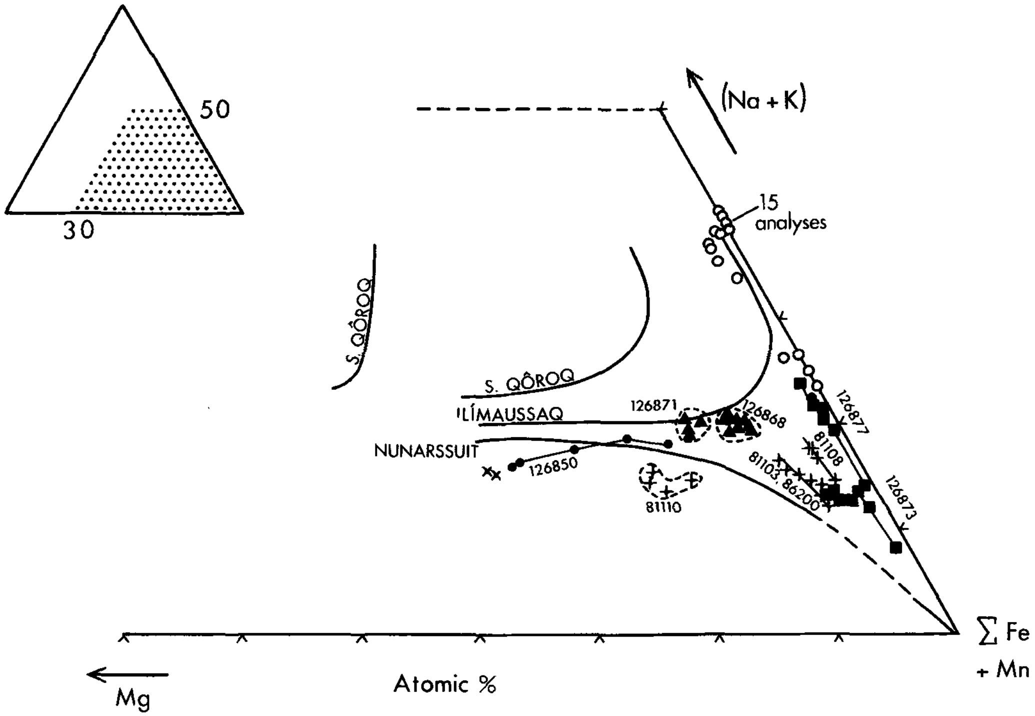

FIG. 5. Amphibole analyses from the Kûngnât Complex. Symbols as for fig. 3*a*. Trends from certain individual rocks are indicated, the starting points of which may be related to the ends of their respective pyroxene trends (fig. 3*a*). The contrast is well seen between trends towards alkali enrichment from silica-undersaturated suites (South Qôroq, Stephenson, 1973 and Ilímaussaq, Larsen, 1976) and trends towards alkali depletion from silica-oversaturated suites (Kûngnât and Nunarssuit-Alangorssuaq, Anderson, 1974).

which reaction occurs varies considerably from intrusion to intrusion and even within parts of the same intrusion giving the 'staggered' amphibole trends such as are seen in fig. 5. Similar behaviour was noted by Mitchell and Platt (1978) in comparable ferroaugite syenites of the Coldwell Complex where 'pyroxenes do not have to evolve to a specific composition before they are replaced by primary amphibole as a liquidus phase'.

Within the Gardar Province, amphibole trends in contrast to those of Kûngnât are observed in the South Qorôq Centre (Stephenson, 1973) and Ilímaussaq Complex (Larsen, 1976). In these predominantly silica-undersaturated suites the amphiboles continue the trend of the preceding pyroxenes towards alkali-enrichment and iron-depletion resulting in a hastingsite → katophorite → arfvedsonite series. This is well seen on fig. 5 where generalized trends from South Qorôq and Ilímaussaq are plotted together with one from another oversaturated suite, Nunarssuit (Anderson, 1974) which behaves in a similar manner to Kûngnât. Trends from two oversaturated suites on Tugtutôq island have been described by Rowbotham (1973) who also notes the contrast between Tugtutôq and Ilímaussaq amphiboles. However, whereas the most primitive amphiboles in both Tugtutôq suites conform with those of other oversaturated suites in being of ferro-edenite to ferro-actinolite or calcic ferro-richterite composition; the majority of amphiboles in these suites are more alkaline, forming a ferro-richterite → alkali ferro-richterite → arfvedsonite → riebeckite-arfvedsonite series. In one of the suites (Tugtutôq Younger Giant Dyke Complex—see also Upton and Thomas, 1980) there is a sharply defined compositional gap between ferro-richterite and riebeckite-arfvedsonite comparable with that observed at Kûngnât.

It is notable that if the pyroxene to amphibole reaction occurs early in the crystallization history, the first amphibole to crystallize in both over- and under-saturated suites is hastingsitic. If amphibole stability is prolonged, both types of suite may result in a most-evolved amphibole of arfvedsonite or riebeckite-arfvedsonite composition. It is between these compositional extremes that the contrasting trends occur: constant alkali enrichment via katophorite compositions in the undersaturated suites; and in the oversaturated suites, iron-enrichment with only slight alkali enrichment or alkali depletion towards edenite and ferro-richterite to ferro-actinolite, followed by rapid alkali enrichment. When considered in such terms the contrast in amphibole trends is very similar to that seen in the pyroxene trends.

Two contrasting amphibole trends are established. Whether or not they may be assigned rigidly to over- and under-saturated suites is more questionable. Exceptions are known, such as the amphiboles from the just-saturated syenites of Klokken (Parsons, 1979) which behave like those from the undersaturated complexes with a sodic hastingsite to ferro-edenite → katophorite → arfvedsonite trend. Neumann (1976) records differing hornblendic amphibole series from over- and under-saturated plutonic members of the Oslo Province, which she attributes to silica activity control. In the development of alkali amphiboles, however, it is generally clear that, as with the alkali pyroxenes, silica saturation is not an overriding influence and is more likely to be a related factor.

In the Coldwell Complex, Ontario (Mitchell and Platt, 1978), two contrasting amphibole series, similar to those of the Gardar suites, occur within the same intrusion: hastingsite → ferro-edenite → ferro-actinolite in the 'Lower Series'; and katophorite → ferro-richterite → arfvedsonite in the 'Upper Series'. Mitchell and Platt attribute this to the development of a peralkaline residual liquid which accumulated in the Upper Series but which was excluded from the Lower Series due to crystal compaction. It is thus implied that alkali enrichment in the amphiboles is controlled, as in the pyroxenes, by the stage at which residual liquids become peralkaline. In general, this is more likely to occur, or will occur earlier, in silica-undersaturated suites than in silica-oversaturated suites. Some over-saturated suites, such as the Tugtutôq trachytic (microsyenitic) to comenditic dykes, are thoroughly peralkaline and produce unusually alkaline pyroxenes and amphiboles, whilst still preserving more typical 'oversaturated' early amphiboles (Rowbotham, 1973); others do not develop peralkaline residua or do so only at a late stage (e.g. Kûngnât). Such a theory can also explain apparent anomalies such as Klokken, which exhibits a 'normal' oversaturated pyroxene trend followed by an alkali-enriched amphibole trend, which could be produced if a peralkaline interstitial liquid developed after the pyroxene to amphibole reaction.

Considerations of stoichiometry and likely coupled substitutions, with the aid of figs. 6 and 7, lead to the following explanations of the divergent trends.

In both oversaturated and undersaturated magmas the initial amphibole substitutions are similar to those of the preceding pyroxenes, i.e.

$$\mathrm{Mg}^{Y} \rightarrow \mathrm{Fe}^{2+Y} \qquad (1)$$

$$\mathrm{Ca}^{X} + (\mathrm{Mg,Fe}^{2+Y}) \rightarrow \mathrm{Na}^{X} + \mathrm{Fe}^{3+Y} \qquad (2)$$

However, in undersaturated suites (South Qôroq, Ilímaussaq) both Na and Si/Al in the amphiboles increase with further fractionation suggesting the substitution:

$$\mathrm{Ca}^{X} + \mathrm{Al}^{Z} \rightarrow \mathrm{Na}^{X} + \mathrm{Si}^{Z} \qquad (3)$$

which, when coupled with (1) and (2) produces a trend from hastingsite, through katophorite to arfvedsonite compositions (Larsen, 1976).

In oversaturated suites (Kûngnât, Nunarssuit) correlations between Al^{Z} and $(\mathrm{Na+K})^{A}$ in the more fractionated compositions (fig. 7*a*), a general fall in (Na + K), and a continuing increase in Si/Al suggest the substitution:

$$(\mathrm{Na,K})^{A} + \mathrm{Al}^{Z} \rightarrow \square^{A} + \mathrm{Si}^{Z} \qquad (4)$$

In such suites the increase in $(\mathrm{Na+K})^{X}$ due to (2) and possibly (3) is slight (cf. poor Na–Ca correlation in fig. 6*c*) compared with the decrease in $(\mathrm{Na+K})^{A}$ due to (4). Consequently a combination of (1) and (4) produces the observed trend from hastingsite, through ferro-edenite towards ferro-actinolite. Note that in both over- and under-saturated suites there is a gradual increase in Si/Al with fractionation from 6/2 to 8/0, which continues the general trend of increasing Si/Al seen in the pyroxenes. In the later (peralkaline) stages of oversaturated suites further substitution may extend the range from ferro-richterite to arfvedsonite:

$$\mathrm{Ca}^{X} + \mathrm{Fe}^{2+Y} \rightarrow \mathrm{Na}^{X} + (\mathrm{Fe}^{3+},\mathrm{Al})^{Y} \qquad (5)$$

possibly followed by the arfvedsonite to riebeckite substitution:

$$\mathrm{Na}^{A} + \mathrm{Fe}^{2+Y} \rightarrow \square^{A} + \mathrm{Fe}^{3+Y} \qquad (6)$$

To summarize, the two amphibole trends may be expressed as:

Silica-undersaturated suites	(1), (2), (3), possibly (6).
Silica-oversaturated suites	(1), (4), (5), (6).

The variation in Al content in the Kûngnât amphiboles explained above results in a wide range in $\mathrm{Al_2O_3}$ from 12.06% in hastingsite from the eastern layered series to 0.71% in ferro-edenite to ferro-actinolite from the western upper layered series. In the eastern syenites there is a slight excess of Al above that required for tetrahedral (*Z*) sites

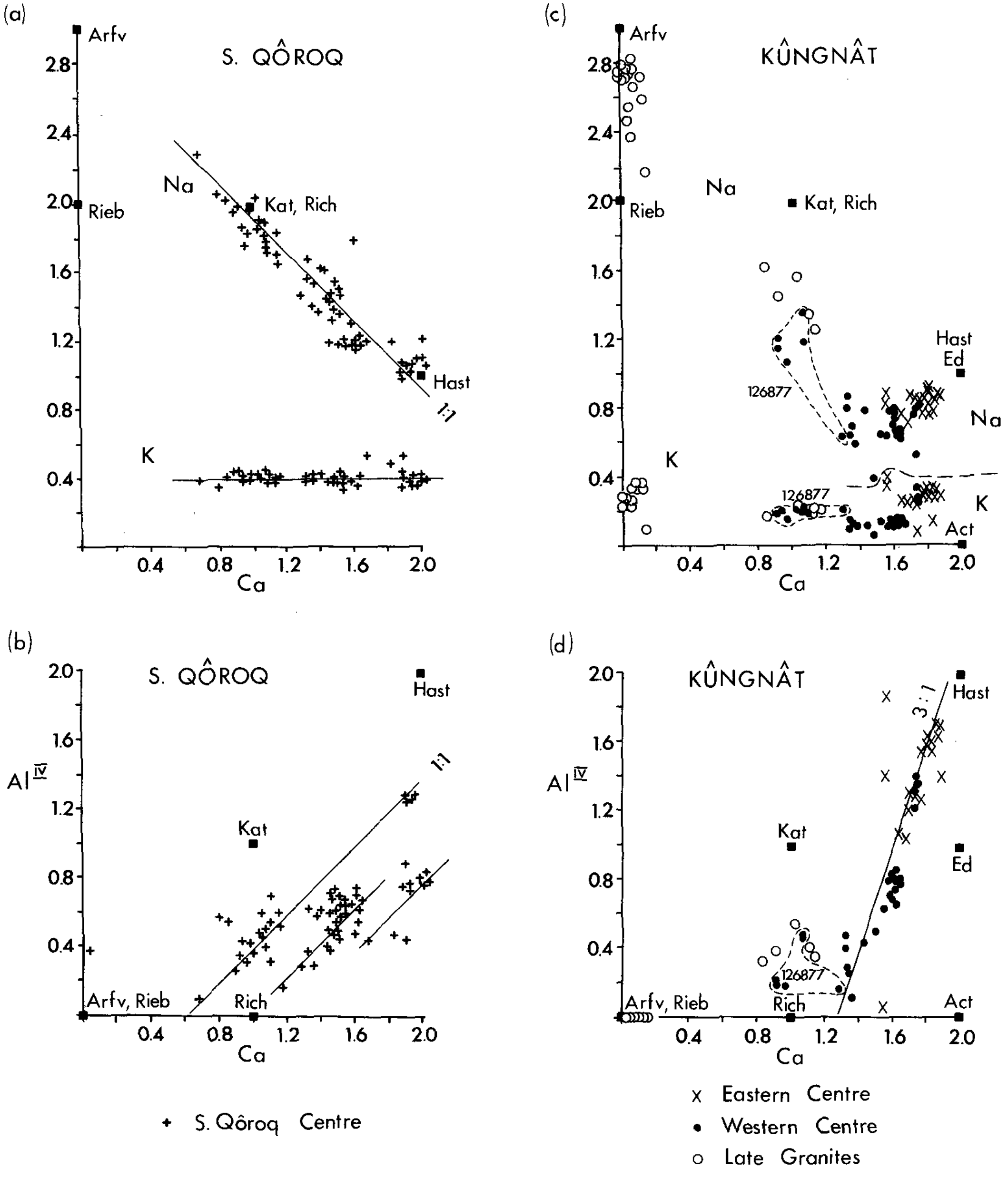

FIG. 6. Contrasting behaviour of Na, K, and Al^{IV} relative to Ca in amphiboles from the silica-undersaturated South Qôroq Centre (Stephenson, 1973) and the silica-oversaturated Kûngnât Complex. See text for details. NB. South Qôroq plots are based upon partial analyses and are therefore plotted as un-normalized atomic proportions. This, together with systematic errors in the Si determinations from different samples, accounts for the presence of several parallel trends in the South Qôroq Ca *vs.* Al^{IV} plot ($Al^{IV} = 8 - Si$), fig. *6b*. End-member compositions are Actinolite (Act), Arfvedsonite (Arfv), Edenite (Ed), Hastingsite (Hast), Katophorite (Kat), Richterite (Rich), and Riebeckite (Rieb). Positions of end-members in figs. *6a* and *6c* are based upon total alkalis (Na + K).

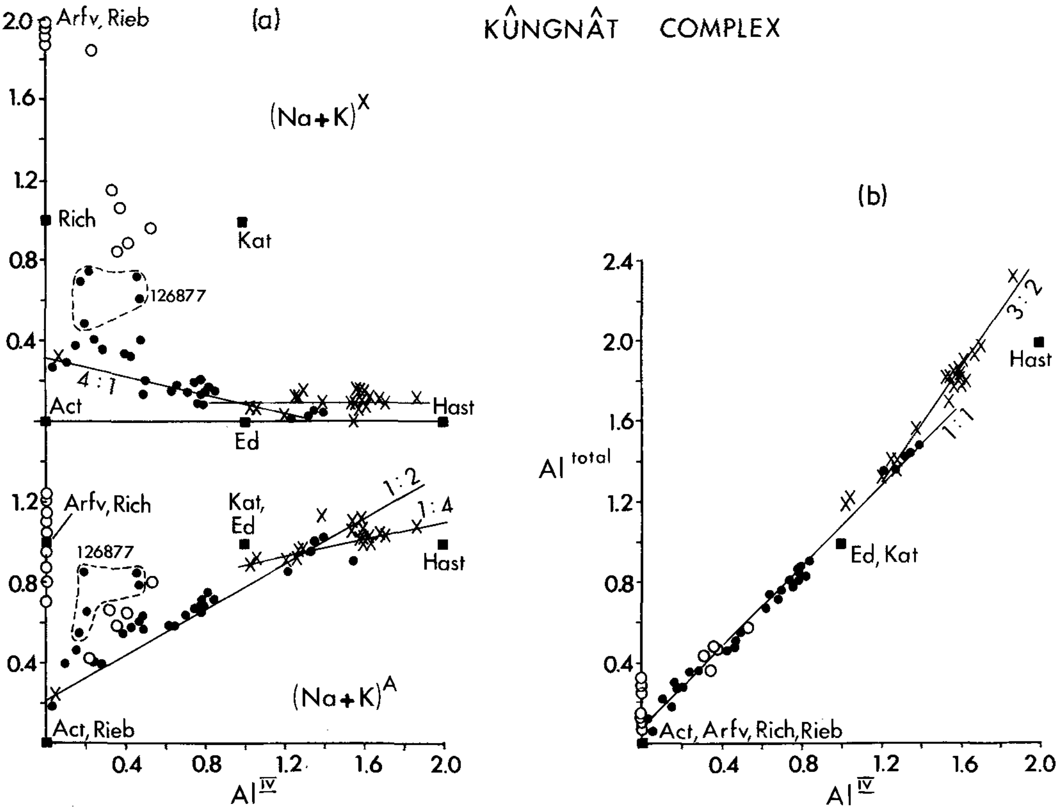

FIG. 7. (*a*) Partitioning of alkalis (Na+K) between A and X sites in Kûngnât amphiboles relative to tetrahedral-coordinated Al^{IV}. (*b*) Total Al *vs.* Al^{IV} in Kûngnât amphiboles, showing slight Al excess at both ends of the trend, indicative of small amounts of octahedral-coordinated Al, probably in *Y*-sites. Symbols and end-members as in fig. 6.

(fig. 7*b*) indicating slight substitution into octahedral sites in the more hastingsitic compositions. Al also enters octahedral (*Y*) sites in arfvedsonites of the late granites which contain up to 1.76% Al_2O_3, corresponding to 0.33 atoms. The remaining 0.66 trivalent atoms necessary to balance the arfvedsonite formula are presumed to be Fe^{3+Y}. In slightly later (lower temperature) aegirine-bearing microgranites, the amphiboles tend towards riebeckite to arfvedsonite with consequent reduction in Al^Y (min. 0.13% Al_2O_3), Na^A and Ca^X. The generally low value of octahedral Al in pyroxenes and amphiboles lends support to the contention that crystallization occurred at relatively high crustal levels. TiO_2 shows a similar variation to Al_2O_3, reducing from 2.31% to 0.11% through the main layered series. In the arfvedsonites and riebeckite arfvedsonites it rises from 0.53 to 1.40%.

Two complete wet chemical analyses of the riebeckite to arfvedsonite from late granite sheets indicate significant concentrations of Li_2O (0.28–0.43%) and F (1.31–2.24%). Cl has not been detected. This concurs with the findings of Rowbotham (1973) that F replaces (OH) to a large extent in riebeckite amphiboles of Si-oversaturated suites, up to at least 1 atom per formula unit.

Biotites. Biotite occurs in all the rocks from gabbro to quartz syenite but appears to show a reaction relationship with riebeckite amphibole in the granitic sheets of western Kûngnât and is absent from slightly lower temperature microgranites. It was, however, stable in late transgressive microgranite sheets of eastern Kûngnât. In the more basic rocks of the ring-dyke suite, eastern syenites and lower western layered series, biotite occurs most commonly as late reaction fringes (possibly sub-solidus) around Fe-Ti oxides. However, in the more fractionated rocks it also occurs as an intercumulus phase in a similar manner to amphibole.

Since Fe^{3+}, H_2O and F have not been determined for the Kûngnât biotites, the analyses have been recalculated to 22 oxygens and variation may be considered in relation to total Fe only. However, in consideration of the environment of crystallization and optical properties of the biotites (Upton, 1960) it seems reasonable to suppose that a significant amount of Fe is as Fe^{3+} and the biotites are more correctly termed lepidomelanes. Fig. 8 shows a wide range of compositions from almost phlogopite (annite$_{31}$) in a ring-dyke gabbro to almost pure annite (annite $_{98.5}$) in granite sheets. Biotites from the ring-dyke suite exhibit a wide range between samples (annite$_{31 \text{ to } 69}$) although individual samples are restricted to a variation of about 10% annite. Intermediate compositions are found in a sample from the eastern border group and compositions from both eastern and western layered series are restricted to the range annite$_{85 \text{ to } 97}$. Compositions from late granites range from annite$_{88.5 \text{ to } 98.5}$. Zoning is slight (maximum 3% annite) and is usually reversed except in the western syenites which show very slight normal zoning.

Apart from the Fe–Mg substitution, other elements show slight variation through the suite (fig. 8). Mn increases with Fe from below detection limits in the ring-dyke suite biotites to widely scattered values with a maximum of 0.43% MnO in biotites from the syenites. Three biotite analyses from a mafic lens in a composite granite sheet are more Mn-rich with up to 0.82% MnO. Alkalis show a slight decrease from ring-dyke to syenite, but increase significantly in the biotites from the composite granite sheet. Si, Al, and Ti are nearly constant in the ring-dyke suite but then show a small, but significant change to higher Si/Al and Si/Ti values in the syenites. This is followed by another 'jump' of similar magnitude to still higher Si/Al in the composite granite sheet. The analyses are almost stoichiometric with $(Na+K)$ ranging from 1.74 to 2.16 and octahedral $(Fe+Mg+Mn)$ very close to 5. $(Si+Al)$ is only slightly less than 8 in the syenites and granites indicating full tetrahedral site occupancy (any deficiency being made up with Ti) and is slightly greater than 8 in the ring-dyke suite implying a little octahedral Al.

Data available from Klokken (Parsons, 1979) and the Tugtutôq Younger Giant Dyke Complex (Upton and Thomas, 1980), indicate very similar suites of biotites. The Klokken suite is almost identical to the Kûngnât suite in terms of Fe/Mg range while both fall within the broader range (annite$_{25}$ to annite$_{98}$) of the Tugtutôq Dyke Complex biotites.

Astrophyllite. Astrophyllite is present in many of the granite and microgranite sheets but seems to be more common and abundant in the slightly earlier, higher temperature granites. It coexists in various combinations with biotite, riebeckite to arfvedsonites, aegirine and zircon. Seven microprobe analyses are available from two separate sheets, two of which are shown in Table II. Compositions are variable in both samples within the general formula $(K,Na)_3(Fe,Mn)_7(Ti,Nb,Zr)_2Si_8(O,OH,F)_{31}$, most variation being in TiO_2(8.71–11.17%), MnO(1.08–2.48%), CaO(0.28–1.10%), Na_2O(2.48–3.83%) and K_2O(2.27–5.67%). Significant amounts of ZnO(max. 0.67%), Nb_2O_3(max. 3.40%), and ZrO_2(max. 1.14%) occur. The coexisting aegirine and riebeckite to arfvedsonite do not show detectable Zr or Nb.

Macdonald and Saunders (1973) include one complete analysis from Kûngnât, comparable with the probe analyses, in which $Fe_2O_3/FeO = 0.02$, $H_2O = 2.60\%$ and $F = 1.24\%$. Minor elements include Ta_2O_5(0.26%), SnO_2(0.30%), PbO(0.37%), and Rb_2O(0.38%). The analysis is very similar to one from the Si-oversaturated Tugtutôq Central Complex but differs from astrophyllite from a pegmatite in the Si-undersaturated Igaliko Complex which contains more Mn, Al, Zr, Ca, and less Nb, Fe^{2+} than the two oversaturated complex examples.

Cryptic variation in the ring-dyke and layered sequences

Other Gardar layered complexes that are compositionally similar to Kûngnât include Nunarssuit (Harry and Pulvertaft, 1963; Anderson, 1974), Klokken (Parsons, 1979), and the Tugtutôq Younger Giant Dyke (Upton and Thomas, 1980). Despite remarkable developments of rhythmic layering in the Nunarssuit syenites and their apparently great thickness, cryptic layering appears to be negligible. Whereas the 600 m main layered syenite succession at Klokken does not itself show cryptic variation, interleaved layers of 'granular syenite' collectively display a regular compositional change with fractionation increasing downwards. Parsons has suggested that these granular syenites crystallized against the roof of the magma chamber and were spalled off as sheets which then sank to the chamber floor.

The structurally complex Tugtutôq Younger Giant Dyke is, in part, a layered intrusion which may exhibit up to 3000 m of cumulitic succession. It differs from Kûngnât, Nunarssuit, and Klokken in its generally dyke-like geometry and in its predominantly gabbroic character. It is, however, genetically important in containing a layered succession showing the upward transition from gabbro to syenite.

The closest described analogue to the Kûngnât

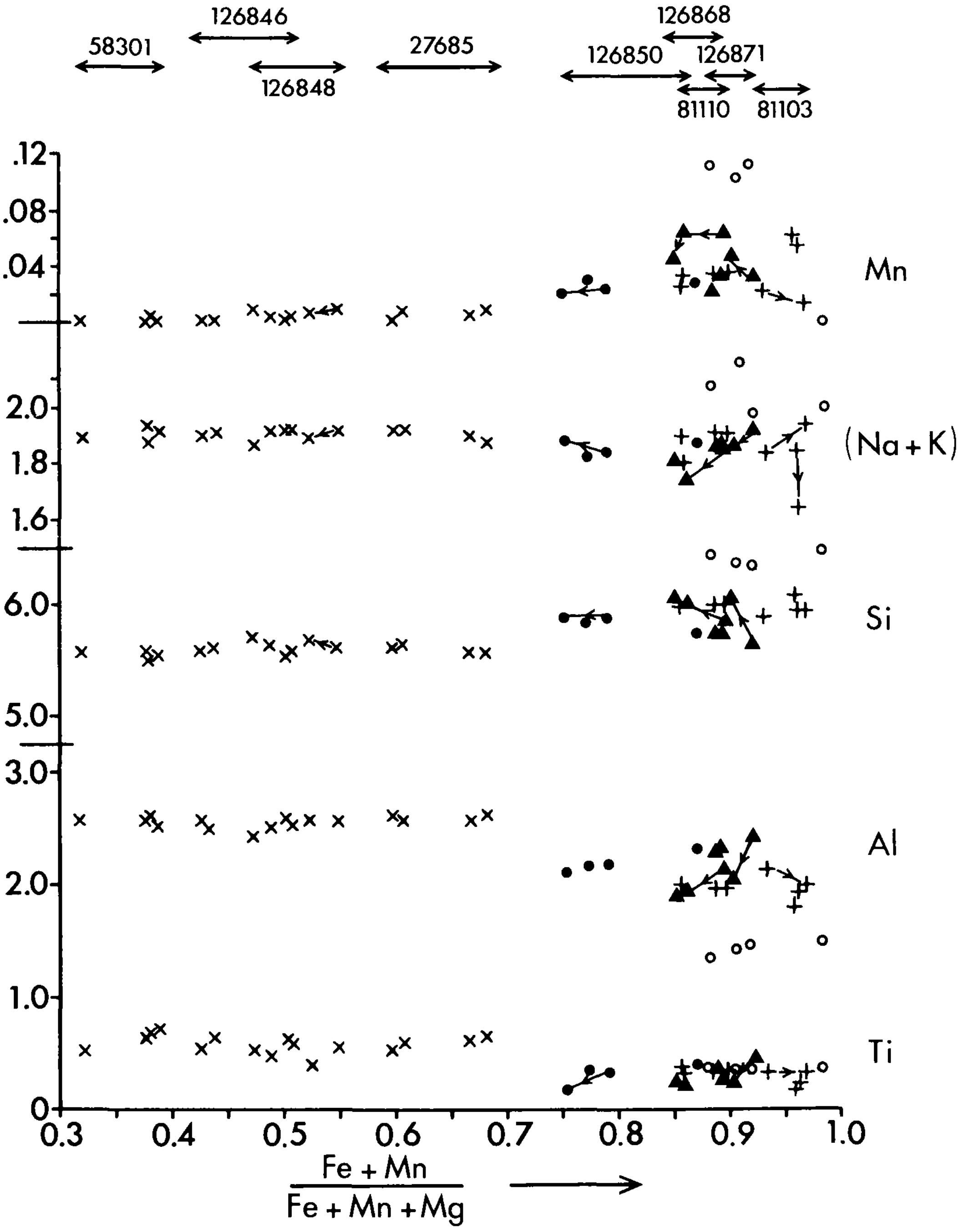

FIG. 8. Biotite analyses from the Kûngnât Complex. Symbols as for fig. 3a. Ranges in (Fe + Mn)/(Fe + Mn + Mg) for individual rocks are indicated. Arrows indicate direction of zoning in individual crystals.

layered syenites may be the 1500 m succession of ferroaugite syenites at Coldwell, Ontario (Mitchell and Platt, 1978). This has been subdivided into a Lower and Upper Series (by the appearance of intercumulus aenigmatite and ferro-richteritic amphiboles). The Lower Series is well layered, with cross-bedding and 'trough-banding' with an upward decrease in the frequency of mafic layers. In these features, as in its mineralogy, it affords a close parallel to the Kûngnât western lower layered Series.

The layered syenites of the two main centres at Kûngnât have little compositional overlap and hence together may be considered as constituting a layered sequence of about 3500 m (1800 m western centre + 1700 m eastern centre). The composition of the mafic syenites of the eastern centre continues the trend shown by the ring-dyke suite.

The mineral trends already described from the gabbro-syenite sequence are smooth and continuous with no compositional breaks. This contrasts with the wide break in olivine compositions between gabbros and syenites at Klokken (Parsons 1979) and also in the silica-undersaturated South Qôroq Centre (Stephenson, 1974). The only significant departure from this pattern occurs in the biotites where Si, Al, and Ti values show a slight jump between gabbro and syenite compositions. Such a jump is not observed at Klokken. Amphiboles do not form a single colinear trend since their starting compositions are governed by the composition of the immediately-precipitating pyroxene. However subsequent amphibole evolution in all rocks proceeds via identical coupled substitutions towards a similar final composition.

The most significant variation in all the mafic silicates is the regular increase in Fe/Mg throughout the series. In the more fractionated pyroxenes this is coupled with an increase in Na but the latter trend is reversed in the later stages of crystallization when amphiboles show a decrease in (Na + K). Although individual biotite crystals show slight reversed zoning, the overall biotite trend is 'normal' with Fe/Mg increasing in sympathy with Fe/Mg in the other mafic phases throughout the series (with the exception of two samples from the eastern layered series which may not be representative). This is in marked contrast to biotites from the Klokken gabbros which show an inverse Fe/Mg relationship with the other phases. Pyroxenes, amphiboles and biotites from Kûngnât all show increasing Si culminating in total tetrahedral site occupancy with a corresponding decrease in tetrahedral Al.

The ring-dyke suite includes a wide range of bulk-rock and mineral compositions. While this is particularly noticeable in the olivines, biotites, and feldspars, the pyroxenes, by contrast, show a relatively short range of compositions. Despite the wide compositional variations, no systematic lateral or vertical changes have been detected within the ring-dyke, except that the most primitive compositions occur in the northwestern sector and that an isolated section of dyke which separates the eastern and western centres contains phases which are considerably more fractionated than those of the main ring-dyke.

Cryptic variation is best seen in the two layered series. In order to quantify this variation it is necessary to establish a measure of structural height for each sample. Because of the basinal stratification within each centre, simple topographic height is not valid, particularly in marginal areas. An attempt has been made to plot each sample upon a generalized cross section similar to fig. 1 in terms of height above sea level and distance from margin (measured perpendicular to the strike of any layering and allowing for the outward dip of the contact). Structural height is then measured perpendicular to the layering upwards from the estimated lowest exposed level. For the western centre this exercise was performed using the sections of Upton (1960, figs. 7 and 8) and a similar generalized scale section was constructed for the eastern centre. The eastern border group was included in this construction, although, owing to the steep dip of the layering in this group, structural height correlates closely with lateral distance from the margin.

Compositional variation of each mafic phase is plotted against structural height in fig. 9. The most magnesian olivine and pyroxene cores are plotted for each sample to remove, so far as is possible, the effect of intercumulus growth. Amphibole and biotite are interpreted as wholly intercumulus; the most magnesian composition of each may record the fractionation state at the commencement of intercumulus growth. The complete ranges of compositions are shown by horizontal lines.

As in most Gardar suites, the pyroxenes show the most complete and ordered trend and hence give the best indication of overall evolution (cf. Stephenson, 1972, Larsen, 1976, Parsons, 1979, Upton and Thomas, 1980). Olivine and amphibole trends are incomplete since these minerals were not present in many of the analysed sections. Biotite too was only analysed from a few representative samples. The two layered series show good correlations of compositions with structural height and can be seen to constitute a complete sequence with only slight compositional overlap between eastern and western centres. Fig. 9 also suggests that there is overlap between the upper and lower series of the western centre (separated by the xenolithic

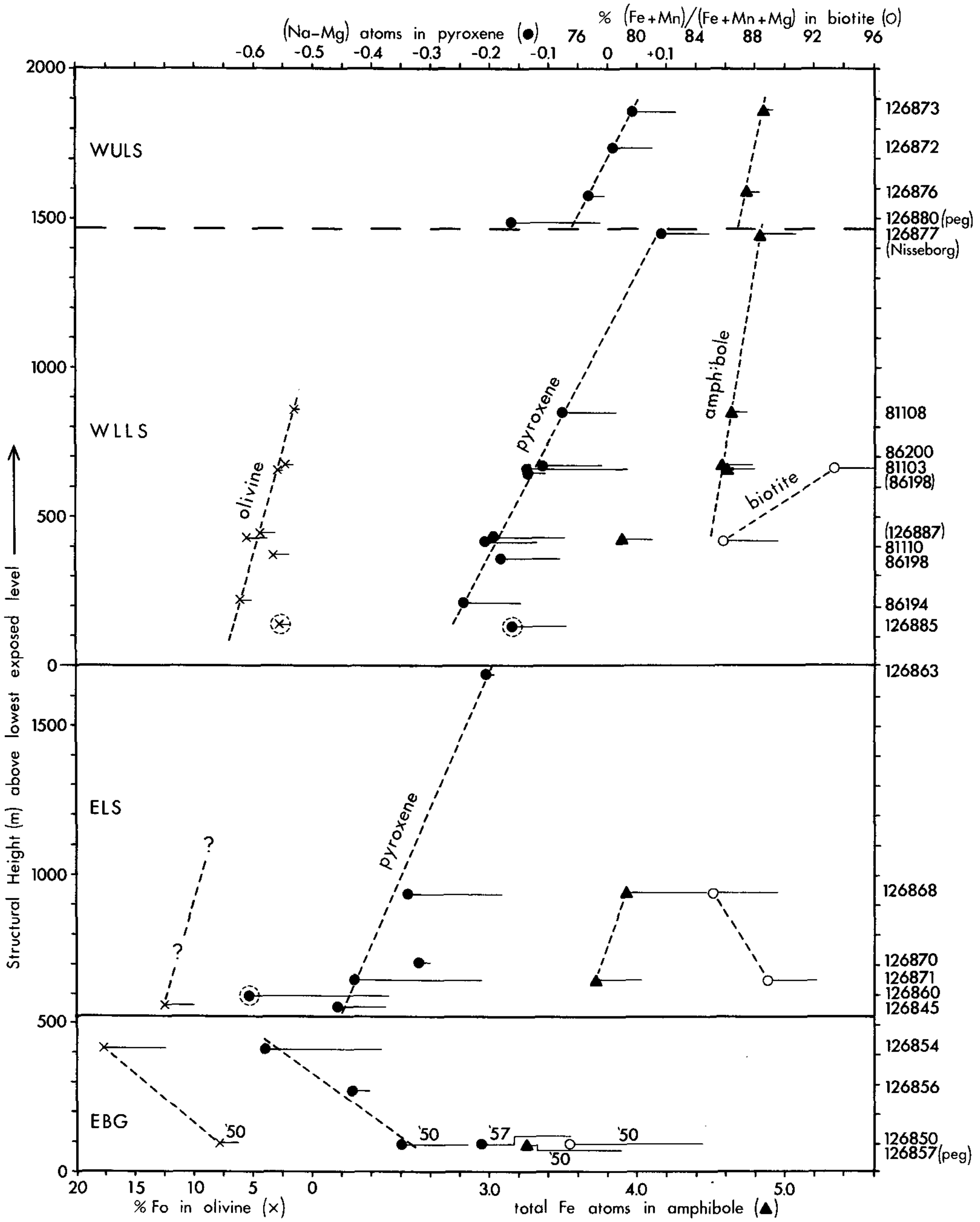

FIG. 9. Variations with structural height in the Kûngnât Layered Series of olivines, pyroxenes, amphiboles, and biotites. For each sample, the most magnesian composition of each phase is plotted with horizontal lines to indicate the full compositional range. Sample numbers in brackets are of uncertain structural height, but olivine and pyroxene compositions provide independent estimates which are in close agreement. Sample 126877 from Nisseborg is located at the base of the Western Upper Layered Series according to the map of Upton (1960) but seems better fitted to the top of the Lower Layered Series on this diagram.

gneiss raft), although this is based solely upon sample 126877 which is from an area (Nisseborg) of doubtful affinity, which may belong to either the lower or upper layered series. Despite these overlaps the pyroxene compositions exhibit a remarkably constant variation with 'stratigraphical height' throughout both eastern and western centres. It may also be significant that olivines and pyroxenes in the western centre show a very similar variation per metre indicating a similar rate of Fe–Mg substitution in both phases.

The eastern border group shows a similar compositional range in most phases to the eastern layered series but the variation is inverted, in that compositions of olivine and pyroxene become more fractionated towards the outer margin which is effectively downwards in the steepened layered sequence (see fig. 1). This may be due to marginal accumulations of volatiles, indicated by an abundance of pegmatitic areas within the eastern border group (Upton, 1960), which would enable stabilization of phases at lower temperatures closer to the margin. The anomalous variation between the two biotite analyses from the eastern layered series has already been noted.

The original model for the formation of the Kûngnât syenites (Upton, 1960) invoked crystal settling in the presence of convective overturn; convection was postulated to have been at its most vigorous following episodes of roof-collapse that exposed the magma body to regions of colder country rock and hence giving rise to enhanced thermal gradients. Clearly, in the light of recently introduced concepts concerning the generation of cumulates (e.g. McBirney and Noyes, 1979), the precise mechanisms involved in the production of rhythmic layering at Kûngnât require re-evaluation. This paper serves merely to quantify some of the mineral variations at Kûngnât in the context of recent studies elsewhere in the Gardar province. The cryptic variations described above strongly support the view that the Kûngnât syenite stocks consolidated from the 'floors' upward. If downgrowing roof zones (upper border groups) with inverted cryptic layering (cf. Klokken; Parsons, 1979) were ever present they would have been removed by erosion except for possible relicts which may have been preserved beneath the (inaccessible) gneiss rafts in the western centre.

Acknowledgements. Fieldwork and systematic sampling for this investigation were initially carried out by B.G.J.U. (with the assistance of C. H. Emeleus, *et al.*), as part of the regional mapping programme by the Geological Survey of Greenland. Further fieldwork by D.S. was made possible through financial support from the University of Western Ontario and the organization of R. C. O. Gill, whose assistance is gratefully acknowledged. Analytical work was supported by the University College of Swansea and microprobe facilities were made available by the Universities of Edinburgh and Durham, through the help and co-operation of P. G. Hill, B. Jeffries and A. Peckett. We have benefited from much useful discussion with many 'friends of the Gardar', in particular J. G. Anderson, A. D. Chambers, C. H. Emeleus, and I. Parsons. The work is published by permission of the Director of the Geological Survey of Greenland.

REFERENCES

Anderson, J. G. (1974) *The geology of Alangorssuaq, Northern Nunarssuit complex, S. Greenland.* Unpubl. Ph.D. thesis, Univ. of Aberdeen.

Bailey, D. K. (1969 *Am. J. Sci.* **267**A, 1–16.

Blaxland, A. B. (1976) *Geochronology and isotope geochemistry of the Gardar alkaline complexes.* Unpubl. Ph.D. thesis, Univ. of Edinburgh.

Blaxland, A. J., van Breemen, O., Emeleus, C. H., and Anderson, J. G. (1978) *Geol. Soc. Am. Bull.* **89**, 231–44.

Bridgwater, D., and Harry, W. T. (1968) *Bull. Grønlands geol. Unders.* **77** (*Meddels. Grønland* **185**).

Chambers, A. D. (1976) *The petrology and geochemistry of the North Qôroq Centre, Igaliko Complex, South Greenland.* Unpubl. Ph.D. thesis, Univ. of Durham.

Charles, R. W. (1975) *Am. Mineral.* **60**, 367–74.

Cox, K. G., Bell, J. D., and Pankhurst, R. J. (1979) *The Interpretation of Igneous Rocks.* Allen & Unwin, London.

Emeleus, C. H., and Upton, B. G. J. (1976) *The Gardar period in southern Greenland.* In Escher, A., and Watt, W. S. (eds.) *Geology of Greenland.* Copenhagen: Grønlands Geol. Unders.

Ernst, W. G. (1962) *J. Geol.* **70**, 689–736.

——(1966) *Am. J. Sci.* **264**, 36–65.

Harry, W. T., and Pulvertaft, T. C. R. (1963) *Greenland Geol. Surv. Bull.* **36** (Meddels. Grønland **169**).

Jones, A. P. (1980) *The petrology and structure of the Motzfeldt Centre, Igaliko, South Greenland.* Unpubl. Ph.D. thesis, Univ. of Durham.

Larsen, L. M. (1976) *J. Petrol.* **17**, 258–90.

McBirney, A. R., and Noyes, R. M. (1979) Ibid. **20**, 487–554.

Macdonald, R., and Saunders, M. J. (1973). *Mineral. Mag.* **39**, 97–111.

Mitchell, R. H., and Platt, R. G. (1978) *J. Petrol.* **19**, 627–51.

Nash, W. P., and Wilkinson, J. F. G. (1970) *Contrib. Mineral. Petrol.* **25**, 241–61.

Neumann, E. R. (1976) *Lithos* **9**, 85–109.

Parsons, I. (1979) *J. Petrol.* **20**, 653–94.

Powell, M. (1978) *Lithos* **11**, 99–120.

Rowbotham, G. (1973) *Hydrothermal synthesis and mineralogy of the alkali amphiboles.* Unpubl. Ph.D. thesis, Univ. of Durham.

Simkin, T., and Smith, J. V. (1970) *J. Geol.* **78**, 304–25.

Stephenson, D. (1972) *Lithos* **5**, 187–201.

——(1973) *The petrology and mineralogy of the South Qôroq Centre, Igaliko Complex, South Greenland.* Unpubl. Ph.D. thesis, Univ. of Durham.

——(1974) *Lithos* **7**, 35–41.

Sweatman, T. R., and Long, J. V. P. (1969) *J. Petrol.* **10**, 332–79.

Upton, B. G. J. (1960). *Bull. Grønlands geol. Unders.* **27** (*Meddels. Grønland* **123**).

——and Thomas, J. E. (1980) *J. Petrol.* **21**, 167–98.

————and Macdonald, R. (1971) *Lithos* **4**, 163–84.

[*Manuscript received 20 April 1981;*
revised 29 September 1981]